

as described [J. Lukas, G. Draetta, J. Bartek, *Eur. J. Biochem.* **207**, 169 (1992)].

21. Mouse monoclonal antibodies to Cdc25A (DCS-122, DCS-124), Cdc25B (DCS-162, DCS-164), and Cdc25C (DCS-193) were generated by standard hybridoma technology. Monoclonal antibody F-6 to Cdc25A was from Santa Cruz and C23420 to cyclin B1 was from Transduction Laboratories. Rabbit antisera to Cdc25A (SC-7157) and Cdc25C (SC-327) were from Santa Cruz Biotechnology, antiserum to Cdk2 Tyr¹⁵ (219440) was purchased from Calbiochem, and antiserum to Chk1 was provided by S. Elledge. DO-1 monoclonal antibody to human p53 was from Oncogene Science. Mouse monoclonal antibodies 12CA5 to the hemagglutinin epitope, DCS-60 and DCS-61 to p21, 5D4 to cyclin D1

and D2, HE12 and HE172 against cyclin E as well as immunoblotting, immunoprecipitation, immunostaining, and in vitro kinase assays were described [J. Lukas *et al.*, *Genes Dev.* **11**, 1479 (1997); M. Thullberg *et al.*, *Hybridoma* **19**, 63 (2000)].

22. U-2-OS sublines conditionally expressing HA-Cdc25A (U-2-OS/B3C4) or p53DD (U-2-OS/C6) were generated by transfection with the respective transgenes in pBI plasmids as described [J. Lukas, C. Storgaard Sørensen, C. Lukas, E. Santoni-Rugiu, J. Bartek, *Oncogene* **18**, 3930 (1999)]. U-2-OS/C6 cells were microinjected with the Mdm2-Luc reporter plasmid (25 µg/ml) and nonimmune mouse IgG as a microinjection marker. After 18 hours, the cells were fixed and processed for combined anti-mouse immunoglobulin

G and anti-luciferase immunostaining as described [J. Lukas *et al.*, *Genes Dev.* **11**, 1479 (1997)].

23. Conditions for single- and multiple-parameter flow cytometry with a FACSCalibur cytometer (Becton Dickinson) and CellQuest and ModFit software were described [J. Lukas *et al.*, *Oncogene* **9**, 2159 (1994)].

24. Supported by grants from the Danish Cancer Society, the Human Frontier Science Program, the Danish Medical Research Council, and the Alfred Benzon Fund. We thank B. Ducommun, S. Elledge, M. Oren, S. Reed, and C. Ward for plasmids and antibodies and R. J. Schultz (Drug Synthesis & Chemistry Branch, NCI) for UCN-01.

28 January 2000; accepted 29 March 2000

Chromatin-Independent Nuclear Envelope Assembly Induced by Ran GTPase in *Xenopus* Egg Extracts

Chuanmao Zhang^{1,2} and Paul R. Clarke¹

The nuclear envelope (NE) forms a controlled boundary between the cytoplasm and the nucleus of eukaryotic cells. To facilitate investigation of mechanisms controlling NE assembly, we developed a cell-free system made from *Xenopus laevis* eggs to study the process in the absence of chromatin. NEs incorporating nuclear pores were assembled around beads coated with the guanosine triphosphatase Ran, forming pseudo-nuclei that actively imported nuclear proteins. NE assembly required the cycling of guanine nucleotides on Ran and was promoted by RCC1, a nucleotide exchange factor recruited to beads by Ran-guanosine diphosphate (Ran-GDP). Thus, concentration of Ran-GDP followed by generation of Ran-GTP is sufficient to induce NE assembly.

The NE controls access to chromatin and plays an important role in the regulation of chromosome duplication and gene expression in eukaryotic cells. In higher eukaryotes, the NE is highly dynamic in the cell cycle, being disassembled on entry into mitosis and reassembled around the segregated daughter chromosomes at telophase. The molecular mechanism of NE assembly is largely unknown, but the process can be studied in a cell-free system made from *Xenopus laevis* eggs (1). In this system, NE assembly around chromatin is inhibited by nonhydrolyzable guanosine 5'-triphosphate (GTP) analogues, suggesting the involvement of a GTPase (2–4). One candidate is the multifunctional GTPase Ran (5), which in *Schizosaccharomyces pombe* plays a role in the maintenance of NE integrity at exit from mitosis (6). Disruption of the Ran GTPase cycle by addition of regulators or dominant Ran mu-

tants inhibits the assembly of nuclei competent for DNA replication in *Xenopus* egg extracts (7–11) and perturbs NE structure (10, 12). However, disruption of the Ran GTPase cycle also inhibits chromatin decondensation and the establishment of nucleocytoplasmic transport during nuclear assembly (11), making it difficult to distinguish any direct role in NE formation.

To examine whether Ran plays a role in NE assembly independently of its effects on chromatin, we added glutathione-Sepharose beads coated with Ran proteins produced as fusions with glutathione-S-transferase (GST) (13) to *Xenopus* egg extracts (14). These fusion proteins are functional, because they produce identical effects on nuclear transport and microtubule stability as nonfusion proteins (10, 11, 15). All of the beads coated with wild-type Ran-GDP became surrounded by a continuous membrane detected with the lipophilic dye 3,3'-dihexyloxycarbocyanine (DHCC) after incubation in the extracts (14), whereas beads coated with GST (Fig. 1) or the related GTPases Ras or Rab5 (16) did not attract any lipid vesicles. Transmission electron microscopy (17) showed a complete double membrane crossed by nuclear pore complexes (NPCs) assembled around Ran-

GDP beads, confirming that a NE-like structure was formed (Fig. 1C). To examine the protein components of this NE, we retrieved beads from the extracts and stained nuclear pore complex proteins (nucleoporins) using the monoclonal antibody (mAb) 414 (18). Ran-GDP strongly promoted the association of nucleoporins, which were stained around the periphery of the beads, consistent with the assembly of NPCs (Fig. 2, A and B). Ran-beads also attracted the major lamin protein present in the extracts, lamin B₃ (Fig. 2, C and D). This protein is actively imported and assembled into a lamina after completion of the envelope during nuclear assembly from chromatin (1), suggesting that active protein import occurs into the pseudo-nuclei formed around Ran-beads and that a lamina may be formed.

To confirm that the NE and NPCs formed by Ran-beads were functional, we carried out an import assay using nucleoplasmin, a karyophilic protein containing a nuclear localization signal. Nucleoplasmin was taken up and strongly concentrated in the pseudo-nuclei, but not in control beads (Fig. 2E). In contrast, a fluorescent dextran too large to pass through nuclear pores was excluded from Ran-GDP beads but diffused into control beads (Fig. 4C). To determine if nucleoplasmin was being imported in a regulated manner, we added dominant Ran mutants after the completion of pseudo-nuclear assembly, but before addition of nucleoplasmin. RanQ69L (substitution of glutamine at position 69 by leucine), which is defective in GTP hydrolysis and therefore locked in the GTP-bound form (19), inhibits Ran-mediated nuclear protein import by disrupting the assembly of import complexes (20). This mutant strongly inhibited nucleoplasmin import into pseudo-nuclei assembled by using beads coated with Ran-GDP (Fig. 2F), even though NEs remained intact (16). Nucleoplasmin import was also inhibited by RanT24N (substitution of threonine at position 24 by asparagine), a mutant that is defective in nucleotide binding and probably blocks import by preventing the recycling of import factors (11). We therefore conclude that NE assembled around beads coated with Ran-GDP restricts access of macromolecules but permits the active transport of karyophilic proteins by way of the NPCs.

¹Biomedical Research Centre, University of Dundee, Level 5, Ninewells Hospital and Medical School, Dundee DD1 9SY, Scotland, UK. ²Department of Cell Biology and Genetics, College of Life Sciences, Peking University, Beijing 100871, China.

E-mail: c.zhang@icrf.icnet.uk and p.clarke@icrf.icnet.uk

REPORTS

The nucleotide exchange factor for Ran, RCC1 (21), which binds to chromatin in a complex that may contain GTPases (22, 23), was also strongly concentrated in pseudo-nuclei (Fig. 3, A and B). The binding of RCC1 to Ran-beads was dependent on the nucleotide-bound state of Ran: Beads coated with RanQ69L-GTP bound RCC1 only poorly, whereas beads coated with RanT24N, which forms a stable inhibitory complex with RCC1 (8, 19, 24), accumulated RCC1 nearly as well as wild-type Ran-beads (Fig. 3C). However, both RanQ69L-GTP and RanT24N were unable to form intact NEs, with some binding of vesicles onto the surface of beads coated with the mutants, but without fusion to form continuous membranes that could exclude fluorescent dextran (Fig. 4). Together, these results indicate that RCC1 is recruited to beads specifically by Ran-GDP. They also indicate that the exchange activity of RCC1 is required for vesicle fusion, because RanT24N blocks this step.

To examine directly if RCC1 promotes vesicle fusion, we supplemented extracts containing Ran-GDP-coated beads with RCC1 (Fig. 5). Conversely, we added Ran binding protein 1 (RanBP1), which inhibits nucleotide exchange on Ran and stimulates the hydrolysis of Ran-GTP to Ran-GDP (25), thereby opposing the activity of RCC1. RCC1 accelerated the fusion of vesicles, forming an intact envelope after 30 min of incubation, compared with 60 min in the absence of further additions. In contrast, RanBP1 blocked vesicle fusion, preventing NE assembly even after 90 min of incubation. We conclude that generation of Ran-GTP by RCC1 from Ran-GDP concentrated on beads causes vesicle fusion to form complete NEs. The inability of RanQ69L-GTP to support vesicle fusion suggests that GTP hydrolysis on Ran is also required. This may account for the ability of nonhydrolyzable GTP analogues to block vesicle fusion (2–4).

In summary, beads coated with Ran-GDP form pseudo-nuclei with intact NEs containing functional nuclear pores, providing a potentially useful in vitro model for investigating NE formation, NPC assembly, and the establishment of nucleocytoplasmic transport. Thus, Ran plays a role in NE assembly that is distinct from its effects on chromatin structure and its role in directing nucleocytoplasmic transport. Because *Xenopus* egg extracts contain Ran at a concentration of 1 to 2 μ M, predominantly in the GDP-bound form (20, 24), simply concentrating Ran-GDP on the surface of beads is sufficient to induce NE assembly. In somatic vertebrate cells, reassembly of the NE during telophase coincides with relocalization of Ran to chromatin (15) and stabilization of the interaction of RCC1 with chromatin (16). Consistent with these results, Ran binds to chromatin before RCC1 and before NE assembly in *Xenopus* egg

Fig. 1. Sepharose beads loaded with Ran-GDP induce NE and nuclear pore complex assembly in *Xenopus* egg extracts. (A) Loading of proteins onto Sepharose beads. Proteins bound to 5 μ l of beads loaded with glutathione-S-transferase (GST) or Ran-GDP were separated on a 10% polyacrylamide gel and stained with Coomassie blue. (B) Immunofluorescence detection of Ran (left) and lipid staining by DHCC (right) of beads incubated in *Xenopus* egg extracts for 120 min. DAPI was used to stain Sepharose beads; no DNA was present. The beads have a diameter of \sim 100 μ M, compared with 10 to 20 μ m for nuclei assembled in egg extracts from sperm chromatin. (C) Transmission electron microscopy: panel 1, GST beads alone; panel 2, GST beads incubated in egg extract; panels 3 and 4 and inset, Ran-GDP beads incubated in egg extract. Nuclear pore complexes are indicated by arrows.

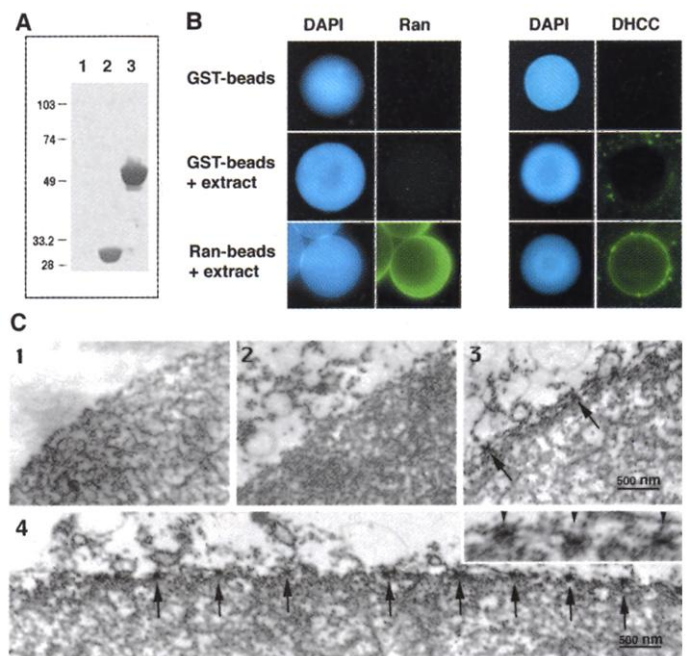
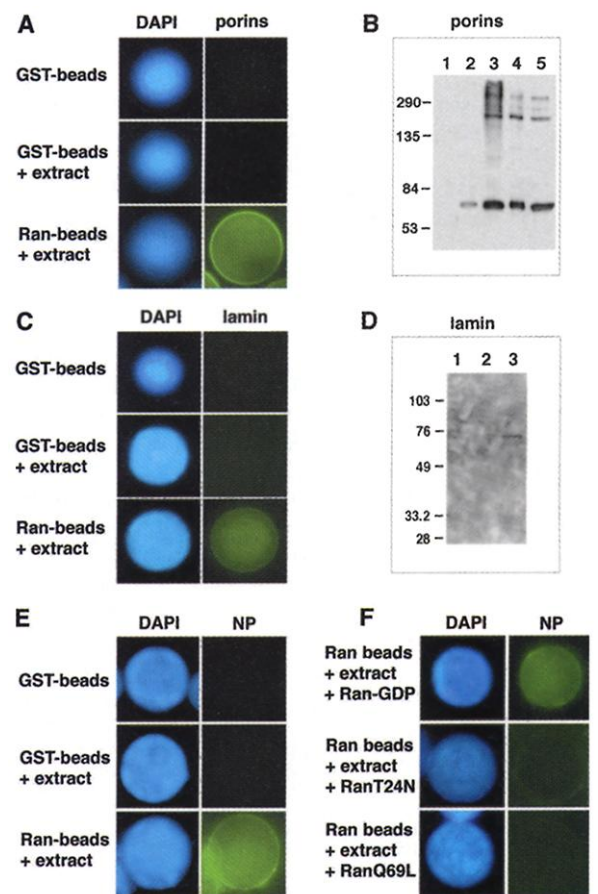
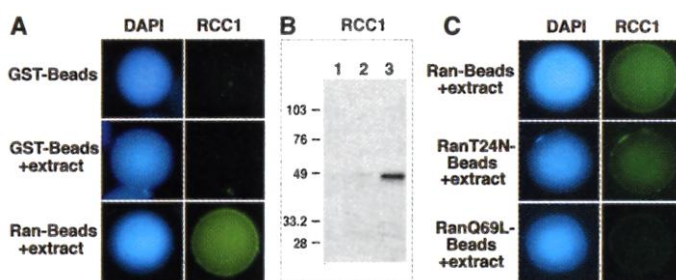


Fig. 2. Pseudo-nuclei formed by Ran-GDP beads incorporate nucleoporins and lamins and actively import nucleoplasmin. (A) Immunofluorescence of nucleoporins detected by mAb 414. (B) Western blotting of nucleoporins detected with the same antibody. Lane 1, GST-beads alone; lane 2, GST-beads incubated in *Xenopus* egg extract; lane 3, Ran-GDP beads incubated in *Xenopus* egg extract; lane 4, nuclei assembled from demembrated sperm chromatin; lane 5, *Xenopus* egg extract. The major nucleoporins detected by mAb 414 in *Xenopus* nuclei are p62, p153, p210, and p340 (Ran binding protein 2). (C) Immunofluorescence and (D) Western blotting of lamin B₃. Lane 1, GST-beads alone; lane 2, GST-beads incubated in *Xenopus* egg extract; lane 3, Ran-GDP beads incubated in *Xenopus* egg extract. Incubations were carried out for 120 min before fixing and centrifuging onto cover slips for immunofluorescence or recovery through a glycerol cushion for Western blotting. (E and F) Import of nucleoplasmin (NP). Nucleoplasmin labeled with fluorescein was added after assembly of pseudo-nuclei for 120 min, and incubation was continued for a further 60 min before fixation and recovery for fluorescence microscopy. (F) Addition of Ran proteins after formation of pseudo-nuclei but before nucleoplasmin addition.



REPORTS

Fig. 3. Ran-GDP recruits RCC1 to beads. (A) Immunofluorescence of RCC1. (B) Western blotting of RCC1 recovered on beads. Lane 1, GST-beads alone; lane 2, GST-beads incubated in *Xenopus* egg extract; lane 3, Ran-GDP beads incubated in *Xenopus* egg extract.



(C) Immunofluorescence of RCC1 bound to beads coated with Ran-GDP, RanT24N-GDP, or RanQ69L-GTP incubated in *Xenopus* egg extract. Incubations were carried out for 120 min before fixing and centrifuging onto cover slips for immunofluorescence or recovery through a glycerol cushion for Western blotting.

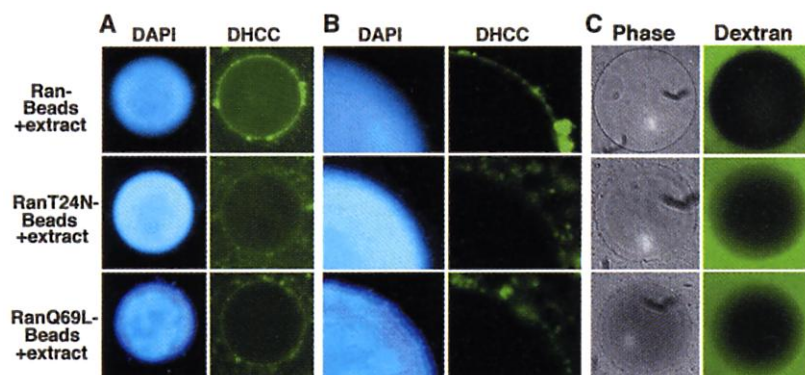


Fig. 4. NE assembly around beads requires functional Ran. (A and B) Lipid staining by DHCC is shown for beads coated with Ran-GDP, RanT24N, and RanQ69L. (A) View of whole beads. (B) Close-up showing continuous membrane staining at the surface of beads coated with Ran-GDP and vesicles at the surface of beads coated with Ran mutants. Incubations were carried out for 120 min before staining. (C) Fluorescent dextran is excluded from Ran-beads but diffuses into beads coated with RanT24N or RanQ69L. Beads were incubated for 120 min in extracts before addition of fluorescein isothiocyanate-dextran (Sigma) and incubation for a further 60 min.

extracts (12, 15). RCC1 alone is not sufficient for NE assembly because beads coated with RCC1 do not form NEs (16). We therefore propose that concentration of Ran-GDP on the surface of chromatin in telophase promotes the binding of membrane vesicles, and then localized generation of Ran-GTP by RCC1 and subsequent GTP hydrolysis on Ran causes vesicle fusion.

Concentration of Ran-GDP promotes NE assembly, whereas Ran-GTP stabilizes microtubule asters and promotes mitotic spindle assembly in *Xenopus* egg extracts arrested in M phase (15, 26–29). A switch in the nucleotide-bound state of Ran from GTP to GDP and relocalization of Ran to chromatin may therefore coordinate NE assembly with disassembly of the mitotic spindle at the end of mitosis.

References and Notes

- I. C. B. Marshall and K. L. Wilson, *Trends Cell Biol.* **7**, 69 (1997).
- A. L. Borman, M. R. Delannoy, K. L. Wilson, *J. Cell Biol.* **116**, 281 (1992).
- J. Newport and W. Dunphy, *J. Cell Biol.* **116**, 295 (1992).
- C. Macaulay and D. J. Forbes, *J. Cell Biol.* **132**, 5 (1996).
- S. Sazer, *Trends Cell Biol.* **6**, 81 (1996).
- J. Demeter, M. Morpew, S. Sazer, *Proc. Natl. Acad. Sci. U.S.A.* **92**, 1436 (1995).
- S. Kornbluth, M. Dasso, J. Newport, *J. Cell Biol.* **125**, 705 (1994).
- M. Dasso, T. Seki, Y. Azuma, T. Ohba, T. Nishimoto, *EMBO J.* **13**, 5732 (1994).
- R. T. Pu and M. Dasso, *Mol. Biol. Cell* **8**, 1955 (1997).
- F. J. Nicolás et al., *J. Cell Sci.* **110**, 3019 (1997).
- M. Hughes, C. Zhang, J. M. Avis, C. J. Hutchison, P. R. Clarke, *J. Cell Sci.* **111**, 3017 (1998).
- C. Zhang, M. W. Goldberg, T. D. Allen, P. R. Clarke, unpublished data.
- Recombinant human Ran proteins were prepared as GST fusions in *Escherichia coli*, purified, and loaded with nucleotides as described (17). Wild-type Ran was loaded with GDP or GTP, RanT24N with GDP, and RanQ69L with GTP. Nucleoplasmin was expressed in *E. coli*, purified, and labeled with 5(6)-carboxyfluorescein-*N*-hydroxysuccinimide ester (FLUOS, Boehringer Mannheim) (17). RCC1 was a gift of A. Wittinghofer (Dortmund).
- Xenopus* egg extracts were prepared as described (17) and then frozen, and samples were stored in liquid nitrogen. Glutathione Sepharose TM 4B beads (100 μ M) (Amersham Pharmacia Biotech), spherical with a mean diameter of \sim 100 μ m, were washed once with 1 ml of phosphate-buffered saline (PBS) and twice with bead buffer [20 mM HEPES-KOH (pH 7.2), 5 mM MgCl₂, 2 mM β -mercaptoethanol]. GST-Ran proteins were loaded onto beads by incubation at 200 μ M in bead buffer for 60 min at room temperature with gentle shaking followed by multiple washes in the same buffer. Protein-loading efficiency was checked on polyacrylamide gels stained

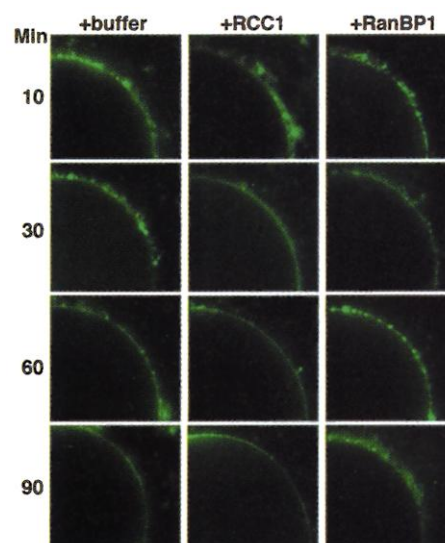


Fig. 5. Regulation of NE assembly by RanBP1 and RCC1. Ran-GDP beads were added to egg extracts, followed by 10 μ M RanBP1 or 10 μ M RCC1. Samples were removed at the times shown, and then stained with DAPI and DHCC; images were captured immediately.

with Coomassie blue or on Western blots with an antibody specific for Ran (17). Pseudo-nuclear assembly was initiated by adding beads (400 per microliter), an adenosine triphosphate-regenerating system, and cycloheximide to the thawed extracts followed by incubation at 23°C. Samples were removed and stained on a slide with DAPI (4',6'-diamidino-2-phenylindole) and DHCC without fixation, and images were taken immediately. For immunofluorescence, samples were fixed for 30 min in 4% formaldehyde [in 10 mM Pipes (pH 7.2), 80 mM KCl, 5 mM EDTA, and 15 mM NaCl]. Beads were then recovered onto cover slips, permeabilized with 0.1% Triton X-100 for 5 min, and prepared for immunofluorescence microscopy with primary antibodies specific for nucleoporins (mAb 414, 1:500), Ran (Transduction Laboratories, 1:100), or RCC1 (Transduction Laboratories, 1:100) as described (17, 15). With the exception of Fig. 5, data shown are for incubations carried out for 120 min. Images were captured on a Zeiss Axioskop microscope with a cooled charge-coupled device camera and processed with Improvision Openlab and Adobe Photoshop software.

- C. Zhang, M. Hughes, P. R. Clarke, *J. Cell Sci.* **112**, 2453 (1999).
- C. Zhang and P. R. Clarke, unpublished data.
- For transmission electron microscopy, extracts containing beads were fixed with 2% glutaraldehyde in PBS overnight at 4°C followed by 1% OsO₄ in PBS for 60 min at room temperature. The samples were then embedded in Spurr's resin and sectioned with a diamond knife. Sections were double-stained with uranyl acetate and lead citrate, then viewed on a 1200 transmission electron microscope (JEOL).
- After incubation in egg extracts, beads were recovered through a cushion of 30% glycerol in sperm nuclear isolation buffer [15 mM tris-HCl (pH 7.6), 60 mM KCl, 15 mM NaCl, 0.5 mM spermidine, 0.15 mM spermine, and 1 mM β -mercaptoethanol]. Proteins were separated on 10% polyacrylamide gels and transferred to nitrocellulose. Blots were blocked with 5% milk powder in Tween-tris buffered saline (TTBS) for 60 min at room temperature and probed overnight at 4°C with primary antibodies specific for nucleoporins (mAb 414, 1:5000), lamin B₃, Ran (Transduction Laboratories, 1:500), or RCC1 (Transduction Laboratories, 1:250). After washing extensively in TTBS, the blots were probed with horseradish peroxidase-coupled anti-mouse or anti-rabbit immunoglobulin G (Bio-Rad) (1:2000 dilution in TTBS,

- 60 min at room temperature) and developed by chemiluminescence.
19. C. Klebe, F. R. Bischoff, H. Ponstingl, A. Wittinghofer, *Biochemistry* **34**, 639 (1995).
 20. D. Görlich, N. Panté, U. Kutay, U. Aebi, F. R. Bischoff, *EMBO J.* **15**, 5584 (1996).
 21. F. R. Bischoff and H. Ponstingl, *Nature* **354**, 80 (1991).
 22. H. Seino, N. Hisamoto, S. Uzawa, T. Sekiguchi, T. Nishimoto, *J. Cell Sci.* **102**, 393 (1992).
 23. A. Lee, R. Tam, P. Belhumeur, T. DiPaolo, M. W. Clark, *J. Cell Sci.* **106**, 287 (1993).
 24. P. R. Clarke, C. Klebe, A. Wittinghofer, E. Karsenti, *J. Cell Sci.* **108**, 1217 (1995).
 25. F. R. Bischoff, H. Kriebler, E. Smirnova, W. Dong, H. Ponstingl, *EMBO J.* **14**, 705 (1995).
 26. R. Carozo-Salas et al., *Nature* **400**, 178 (1999).
 27. P. Kalab, R. T. Pu, M. Dasso, *Curr. Biol.* **9**, 481 (1999).
 28. T. Ohba, M. Nakamura, H. Nishitani, T. Nishimoto, *Science* **284**, 1356 (1999).
 29. A. Wilde and Y. Zheng, *Science* **284**, 1359 (1999).
 30. We thank M. Hughes and F. Nicolás for providing recombinant proteins, and members of our labora-

tory for discussions and preparation of the manuscript. We are grateful to F. R. Bischoff, R. A. Laskey, and A. Wittinghofer for providing reagents. M. Kierans and M. Gruber (Department of Biological Sciences, University of Dundee) provided valuable technical assistance with electron microscopy. Supported by grants from the Biotechnology and Biological Sciences Research Council and the Cancer Research Campaign.

10 December 1999; accepted 6 April 2000

Nipah Virus: A Recently Emergent Deadly Paramyxovirus

K. B. Chua,¹ W. J. Bellini,^{2*} P. A. Rota,² B. H. Harcourt,²
 A. Tamin,² S. K. Lam,¹ T. G. Ksiazek,² P. E. Rollin,² S. R. Zaki,²
 W.-J. Shieh,² C. S. Goldsmith,² D. J. Gubler,³ J. T. Roehrig,³
 B. Eaton,⁴ A. R. Gould,⁴ J. Olson,² H. Field,⁵ P. Daniels,⁴
 A. E. Ling,⁶ C. J. Peters,² L. J. Anderson,² B. W. J. Mahy²

A paramyxovirus virus termed Nipah virus has been identified as the etiologic agent of an outbreak of severe encephalitis in people with close contact exposure to pigs in Malaysia and Singapore. The outbreak was first noted in late September 1998 and by mid-June 1999, more than 265 encephalitis cases, including 105 deaths, had been reported in Malaysia, and 11 cases of encephalitis or respiratory illness with one death had been reported in Singapore. Electron microscopic, serologic, and genetic studies indicate that this virus belongs to the family *Paramyxoviridae* and is most closely related to the recently discovered Hendra virus. We suggest that these two viruses are representative of a new genus within the family *Paramyxoviridae*. Like Hendra virus, Nipah virus is unusual among the paramyxoviruses in its ability to infect and cause potentially fatal disease in a number of host species, including humans.

An outbreak of severe febrile encephalitis associated with human deaths was reported in Peninsular Malaysia beginning in late September 1998. The outbreak was associated with respiratory illness in pigs and was initially attributed to Japanese encephalitis (JE) (1). JE is a mosquito-borne viral disease that is enzootic in the region, and pigs are among the amplifying vertebrate hosts (2). By February 1999, similar diseases in pigs and humans were recognized in other regions in Malaysia, in association with the movement of a large number of pigs from Ipoh southward into the new outbreak areas. In March 1999, a cluster of 11 cases of respiratory and encephalitis illnesses was noted in Singapore

in abattoir workers who handled pigs from the outbreak regions in Malaysia. The outbreak in Singapore ended when the importation of pigs from Malaysia was prohibited, and the outbreak in Malaysia ceased when over 1 million pigs were culled from the outbreak area and immediately surrounding areas (3). A total of 265 cases of encephalitis, including 105 deaths, were associated with the outbreak in Malaysia.

Because some of the epidemiologic characteristics of the disease in humans were distinct from those of JE [most cases occurred in adult males who worked with pigs, very few case patients were young children, and neither mosquito control nor JE vaccination programs appeared to affect the course of the outbreak (4)], investigators in Malaysia expanded attempts to isolate an agent. In early March 1999, Vero cells inoculated with cerebrospinal fluid specimens from three fatal cases of encephalitis developed syncytia.

Electron microscopic (EM) studies of the virus, named Nipah virus (5), demonstrated features characteristic of a virus belonging to the family *Paramyxoviridae* (Fig. 1). This family of viruses typically possesses a single-stranded nonsegmented RNA genome of negative polarity that is fully encapsidated by protein. The helical

nucleocapsid structure is surrounded by membrane derived from the plasma membrane from which the viruses bud. Virus particles vary in size from 120 to 500 nm. The paramyxovirus envelope contains two transmembrane glycoproteins, a cell receptor binding protein [G (glycoprotein), H (hemagglutinin), or HN (hemagglutinin/neuraminidase)] and a separate fusion (F) protein. Thin-section EM studies of infected cells revealed filamentous nucleocapsids within cytoplasmic inclusions and incorporated into virions budding from the plasma membrane (Fig. 1B). Typical "herringbone" nucleocapsid structures, approximately $1.67 \pm 0.07 \mu\text{m}$ in length (Fig. 1A) and with an average diameter of 21 nm, were observed in infected cells by means of negative stain preparations. Extracellular virus particles were pleomorphic, with an average diameter of 500 nm (Fig. 1C). Surface projections (not shown in the figure) along the virion envelope were only sporadically seen by thin-section EM and measured 10 nm in length.

Analysis of representative human and animal specimens from the outbreaks in Malaysia and Singapore provided an etiologic link between the two outbreaks (Table 1). Nipah virus-infected cells reacted strongly with Hendra virus antiserum (6) but did not react with antisera against other paramyxoviruses, including measles virus, respiratory syncytial virus, and parainfluenzaviruses 1 and 3, as well as other viruses, including herpes virus, enteroviruses, and JE virus, as indicated by immunofluorescence antibody assays. Cross-neutralization studies (7) resulted in an 8- to 16-fold difference in neutralizing antibodies between Nipah and Hendra viruses, indicating that the viruses, though related, were not identical.

Serologic studies in which Hendra virus antigen was used for detection of Nipah virus immunoglobulin M (IgM) and IgG (8) suggested that Nipah virus was the principal etiologic agent of the outbreak in Malaysia and Singapore. Virus isolation or serologic testing confirmed Nipah virus infection in all cases from Singapore and in all but one of the initially identified encephalitis cases from Malaysia (Table 1). The most notable illness in pigs implicated in transmitting the virus to humans was respiratory and included a loud and distinctive cough. Although serologic studies found evidence of Nipah virus infec-

¹Department of Medical Microbiology, University of Malaya Medical Center, 50603 Kuala Lumpur, Malaysia. ²Division of Viral and Rickettsial Diseases, National Center for Infectious Diseases (NCID), Centers for Disease Control and Prevention (CDC), 1600 Clifton Road, Atlanta, GA 30333, USA. ³Division of Vector-Borne Diseases, NCID, CDC, Fort Collins, CO 80522, USA. ⁴Commonwealth Scientific and Industrial Research Organisation, Australian Animal Health Laboratory, 5 Portarlington Road, East Geelong, Geelong, Victoria 3220, Australia. ⁵Department of Primary Industries, Animal Research Institute, 665 Fairfield Road, Yeerongpilly, Queensland 4105, Australia. ⁶Department of Pathology, Singapore General Hospital, Outram Road, Singapore 0316.

*To whom correspondence should be addressed.